

Tuning of resonant Zener tunneling by vapor diffusion and condensation in porous optical superlattices

Mher Ghulinyan,¹ Zeno Gaburro,¹ Diederik S. Wiersma,² and Lorenzo Pavesi¹

¹*Nanoscience Laboratory, Department of Physics, University of Trento, Trento, Italy*

²*European Laboratory for Nonlinear Spectroscopy and INFM-MATIS, Sesto Fiorentino, Florence, Italy*

(Received 21 April 2006; revised manuscript received 30 May 2006; published 20 July 2006)

We study a vapor-controlled optical superlattice realized with a silicon-based dielectric mesoporous material. By flowing organic vapors through the nanometer-sized pores, the position dependent refractive index can be continuously tuned, resulting in a tilted photonic band structure. A careful design of pore size distribution, close to the critical radius of capillary condensation of vapor, makes the superlattice sensitive to the flow direction. We drive the optical superlattice to the resonant Zener tunneling condition, introducing an enhanced transmission channel through the photonic crystal. Our results show that vapor capillary condensation can be used to modify the properties of optical superlattices allowing, e.g., to realize fast gas sensing devices due to their advantage to respond to vapor flow fronts.

DOI: 10.1103/PhysRevB.74.045118

PACS number(s): 42.70.Qs, 42.25.Dd, 73.21.Cd, 78.67.Pt

I. INTRODUCTION

The control of optical properties of photonic crystals is currently an active research topic.^{1,2} This is especially important when it can be applied as a function of position inside the crystal, because in such case the photonic energy bands can be tilted or curved.^{3,4}

Dielectric photonic crystals are often fabricated by periodically alternating one or several materials with air voids. With this method effective photonic crystals can be realized within a small volume, potentially allowing integration over a large scale.⁵ There is a second strategic aspect of air voids: they can be filled and emptied. From the point of view of the photonic properties of the structure, the effect of locally controlled fluid exchange is equivalent to a local tuning of the refractive index. The aim of this paper is to demonstrate an effective mechanism to modulate the band structure of photonic crystals *as a function of position*, by filling and emptying air gaps with fluids, taking the advantage of capillary condensation.^{6,7}

The starting idea is to exchange, with the crystal scaffold, vapors close to their dew point. This leads to capillary condensation of the liquid—and a consequent significant modulation of the refractive index n ($\Delta n/n \approx 10^{-2}$)—in all voids whose linear dimension is below a critical value r_c , calculated according to Kelvin-Laplace theory.⁸ For typical solvents in the proximity of dew point, the critical radius of curvature of the liquid-vapor interface r_c , is in the range of few tens of nanometers, i.e., significantly below the characteristic length in optical photonic crystals. This suggests to consider two levels of structuring. The first level—for the fluid exchange control—is a high-resolution structure, which leads to porous elementary building blocks. The pore size distribution, which can be fabricated as a function of position, locally determines the amount of capillary condensation and thus the quantitative shift of the effective refractive index. The second level of structure for the photonic properties can be then independently designed at lower resolution (usually, of the order of one-quarter wavelength). In this paper, we show how the capillary condensation in fine porous struc-

tures can be used to tailor the optical response of a photonic crystal by modifying locally the material refractive index. In particular, we propose a one-dimensional photonic Zener tunnel crystal, which is pushed in and out of resonance by exposing it to vapors of ethanol in proximity of the dew point.⁹

Zener tunneling (ZT) of light waves has been studied and observed in various physical systems, such as optical lattices,¹⁰ waveguide arrays¹¹ and two-dimensional photonic lattices.¹² Photons undergo ZT in a one-dimensional optical superlattice, in which two photonic minibands are tilted to be coupled resonantly.⁴ An optical superlattice can be built by repeating a dielectric supercell “*Mirror/C/Mirror/D*” composed of two cavities *C* and *D* centered at different frequencies and coupled through dielectric mirrors. When a constant optical path is maintained through the structure, two flat high-transmission photonic minibands separated by a frequency minigap, form in the stop band of the optical superlattice (Fig. 1). The introduction of an optical path gradient $\Delta\delta$ along the superlattice growth direction results in a tilted photonic band structure.^{3,4} The optical path gradient, which turns the delocalized photonic bands into Wannier-Stark (WS) ladders¹³, acts in the same way as the electric field in the case of the electrical Zener diode.¹⁴ In close analogy to the case of a semiconductor crystal, in an optical superlattice the light transmission strongly increases¹⁵ at the ZT frequency ω_{ZT} when the photonic minibands couple resonantly at a critical band tilting. This can be seen as an intense point in Fig. 1, when two states of different minibands come to the same frequency and suffer an anticrossing at the critical optical path gradient (successive anticrossings occur upon further increasing the band tilting). The photonic structure can be in condition of resonance [Fig. 2(a), left-hand panel] or not (right-hand panel), depending on the optical path gradient. In the reported photonic ZT structures, the optical path gradient has been hitherto built-in as a fixed parameter, during fabrication.

The paper is organized as follows. In Sec. II we describe the sample design and the preparation technique, followed by the description of the optical transmission measurement

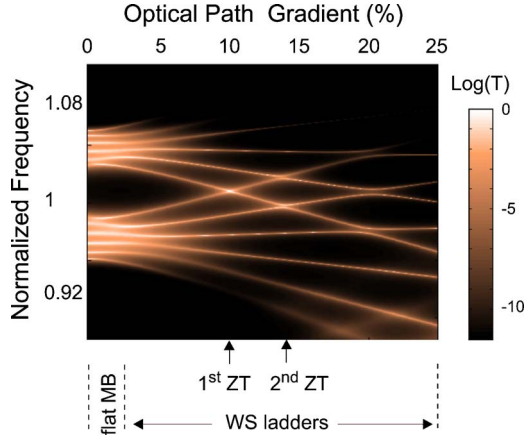


FIG. 1. (Color online) Calculated distribution of transmission T of the optical superlattice as a function of optical path gradient $\Delta\delta$ and normalized frequency ω/ω_{ZT} . Two flat photonic minibands ($\Delta\delta=0$) transform gradually into Wannier-Stark (WS) ladders when the gradient (band tilting) increases. First (1st ZT) and second (2nd ZT) anticrossings of WS states result in resonant light transmission through the superlattice.

setup. In Sec. III we discuss the results of the transmission measurements and the effects of different capillary condensation upon changing the vapor flow direction. In the end of the section we discuss analogies between resonant Zener tunneling through the optical superlattice and the electrical Zener breakdown of the reverse current of electrons in a semiconductor diode. Finally, in Sec. IV we summarize our results and draw conclusions.

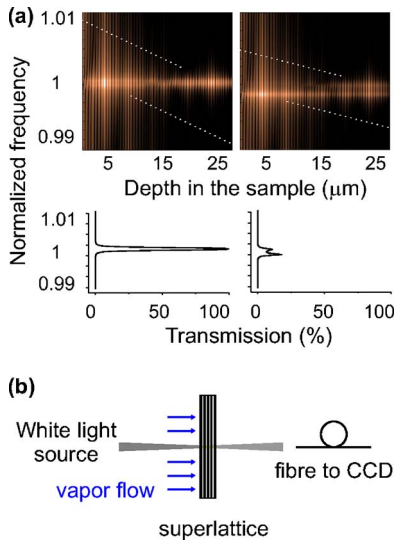


FIG. 2. (Color online) The calculated light intensity distribution inside the optical superlattice, plotted around the normalized frequency ω/ω_{ZT} and versus depth in the sample. Below the corresponding transmission spectra for two cases of resonantly coupled (left-hand panels) and decoupled WS states (right-hand panels) are shown. The dotted lines are a guide for the eye and show the minibands tilting. (b) The sketch of the experimental setup.

II. EXPERIMENT

A. Sample design and preparation

We have grown the optical superlattices by controlled electrochemical etching of Boron doped (100)-oriented silicon wafers with a resistivity between $0.01-0.02\Omega\text{ cm}$. In particular, an etching current density of 50 mA/cm^2 was used to grow both C and D type of cavities, with a resulting 73% porosity (the corresponding nominal refractive indices were $n_C=n_D=1.5$). The different physical thicknesses of the layers were controlled by adjusting the duration of the etch times. $30\text{ }\mu\text{m}$ thick superlattice structures were made free-standing by applying an electropolishing current pulse at the end of the growth process (details on sample preparation are described elsewhere).^{4,16}

A negative optical path gradient, defined as the relative difference between the optical thickness of the first and the last cavity of the same photonic miniband, was achieved by adjusting the duration of the etch stop current between successive layers. The latter controls the final refractive index and, therefore, the optical thickness of each layer. The built-in optical path gradient was adjusted to its critical value $\Delta\delta_{ZT}$ in order to study the modulation of the photonic band structure of superlattices when exposed to organic vapors. The optical parameters of the samples have been designed in order to achieve a maximum tunability range of the superlattice when the vapor exposure is turned on and off. The choice of the ZT frequency ω_{ZT} of the samples determines the set of optical path values of all the coupled cavities through the superlattice (six of each type).¹⁷ In particular, for our samples this implies a value of $\Delta\delta_{ZT}\approx 9\%$ for the optical path gradient.

Since we aim to modify the built-in gradient of the band structure under exposure to vapor, we address below some aspects of vapor capillary condensation in our mesoporous structures. Mesoporous silicon shows a honeycomblike structure with polygonal-shaped cylindrical nonintersecting pores, perpendicular to the substrate.¹⁸ Each particular pore has the length of the photonic structure and, in a self-standing film, is open in both ends. Therefore, one can use Cohan's formula to calculate the critical radius r_c according to the modified Kelvin equation for cylindrical pores open at both ends¹⁹

$$r_c = -\frac{v_m\gamma}{k_B T \ln(S)}, \quad (1)$$

where v_m is the adsorbate molecular volume, γ is the surface tension, T is the temperature, S is the ratio of the actual vapor pressure P to its saturation value P_0 . We select to work with ethanol for its availability, large refractive index ($n=1.362$) and low toxicity. Upon assuming realistic working conditions $S\approx 0.98$ we obtain $r_c\approx 30\text{ nm}$ (for ethanol $v_m=58.43\text{ ml/mol}$, $\gamma=23.00\text{ mN/m}$). By fabricating the sample with average pore size below (above) r_c in the cavities with longer (shorter) optical path, the effectiveness of capillary condensation is maximized (fine tuning is eventually possible by adjusting S during operation). Thus, we

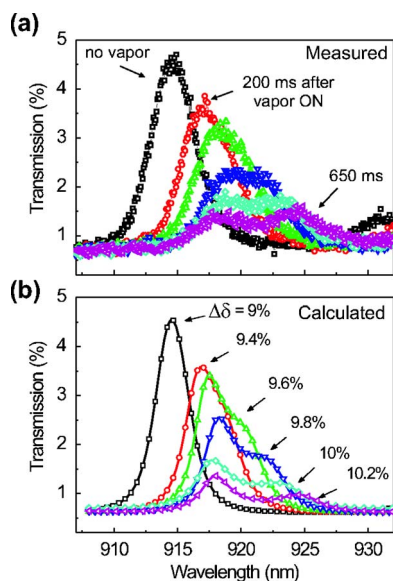


FIG. 3. (Color online) Vapor induced splitting of the Zener tunneling peak. (a) Experimental spectra of the sample exposed to ethanol vapors, (b) transfer-matrix calculations. The original double resonance peak splits in two separate modes when the built-in tilting is modified by the external “field” mimicked by the refractive index gradient induced by the ethanol vapor flow.

adjust the etching conditions for a nominal target pore size distribution in the range $\approx 26 \pm 10$ nm ($\approx 33 \pm 10$ nm) for the cavity with longest (shortest) optical path. The obtained porosity in these conditions is about 68.5% (76%). Since porosity determines the average index n of each layer, the physical thicknesses d of the cavities are then adjusted according to the optical path $n \times d$ required for the built-in gradient. Cavities in-between have been designed with intermediate optical paths.

B. Experimental setup

We have performed transmission measurements, in which an incident white light beam (Tungsten lamp) was focused into a small spot on the sample surface [Fig. 2(b)]. A fiber bunch was placed far from the sample allowing to collect the transmitted signal with a very small numerical aperture ($NA \sim 0.0075$). The signal was sent to a spectrometer interfaced to a cooled silicon charge coupled device (CCD). A flow of ethanol vapor was realized close to the surface of the samples using a gas-controller device. The CCD was triggered by the gas-controller and acquired the transmitted light with a variable delay after the vapor was switched-on.

III. RESULTS AND DISCUSSION

A. Analysis of the measured data

In Fig. 3(a), measured spectra of the optical superlattice under exposure to saturated vapor of ethanol are reported. A ZT peak of resonantly coupled states appears at ~ 914 nm in

the absence of the vapor flux. The other curves, reported in Fig. 3(a), correspond to different snapshots in time after the vapor flux has been started. The splitting of the single tunneling peak into two uncoupled WS states is clearly visible. The observed splitting of the original peak confirms the vapor-induced change in the refractive index gradient and thus a *change in the band tilting*. As expected, the modified gradient drives the sample out of the resonant Zener coupling condition. Moreover, we observe a decrease in the intensity of the peaks, which additionally confirms that the Zener coupling condition is not anymore fulfilled. The observed redshift of the spectra is due to an increased n_{eff} of the layers in the presence of the vapor. Starting with $\Delta\delta_{\text{ZT}} \sim 9\%$ for the ZT condition in this sample [Fig. 3(b)], a maximum increase of the gradient by 1.2% between the first and last cavity layers (total gradient of 10.2%) has been calculated by fitting the experimental data with standard transfer matrix calculations.²⁰

Equation (1) is a static model for the effect of vapor on the photonic band structure. In order to explain the time evolution under nonequilibrium conditions, one must resort to a model for the vapor diffusion process. Indeed, capillary condensation plays an important role also in the diffusion process of vapor. Because of porosity gradients, the molecular diffusion through pores which contain both vapor and adsorbed phases ($r > r_c$), appears to be sensitive to the exposure direction. The Knudsen diffusion constant D_K of the vapor,²¹ which accounts for the collisions of molecules with the pore walls, is a function of pore radius and relative pore filling θ ,²² and can be expressed as $D_K \sim r\sqrt{1-\theta}$. Under nonequilibrium conditions the relationship between D_K and θ becomes intricate by the fact that θ locally depends on the diffusion (i.e., on D_K) in the preceding layers as well.

B. Kinetic series measurements: the effect of vapor flow direction

To test the effect of diffusion, we have performed kinetic series of light transmission through a second sample, under ethanol vapor exposure of both sides, recording spectra with a 30 ms time step. The sample was designed with the same procedure, but slightly off resonance, in such a way that the exposure from one side could be used to push it towards ZT resonance, and from the other to pull it further off resonance. The measurements are reported in Fig. 4(a). Since the average radius of pores changes with depth, vapor condensation in pores with $r < r_c$ and molecular self-diffusion in pores with $r > r_c$ should result in different refractive indices, and thus optical path gradients, depending on the choice of vapor exposure direction. Using the numerical fitting procedure for the measured spectra, the corresponding condensation-induced changes of the refractive index of the cavities, have been extracted.

Two basic parameters, describing the index changes, have been introduced in order to fit the data. The first one, Δn , controls the gradient of the index through the structure and therefore explains the splitting (or coupling) of modes. The

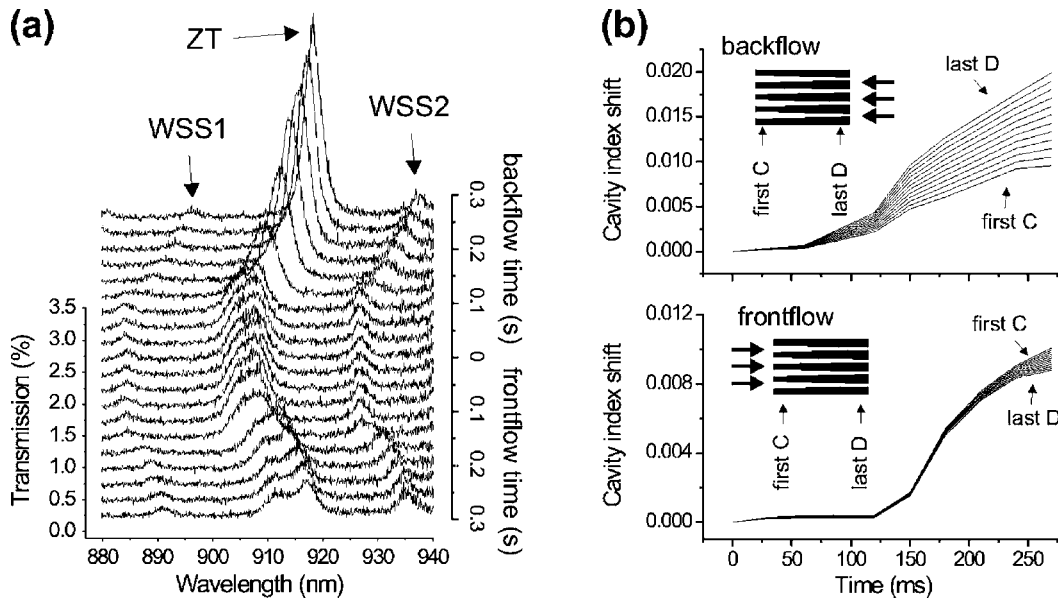


FIG. 4. (a) Kinetic series of light transmission through the optical superlattice. Tuning or detuning of Zener coupling between Wannier-Stark states (WSS) in two minibands can be observed when the vapor flow is sent either to the sample frontside or backside. (b) Due to the pore size gradients through the structure, the vapor-induced refractive index change shows an asymmetric behavior under backside (upper panel) and frontside (lower panel) exposure.

second one, n_{bg} , considers a homogeneous shift of the refractive index through the superlattice and controls the absolute redshift of the spectra. In Fig. 4(b) the refractive index shift ($\Delta n + n_{bg}$) from the original value in all 12 cavities is plotted in the case of frontside (upper panel) and backside (lower panel) vapor flow. Both qualitative and quantitative differences between the two cases are appreciable. The absolute vapor-induced difference between the first and last cavity index is almost 10 times higher in the case of the backside exposure. The transfer-matrix calculations show that the change in the optical path gradient is $\geq 1\%$ and 0.1% at backside and frontside exposures within 270 ms, correspondingly. These observations confirm the different scenarios for frontside and backside vapor exposures in an optical superlattice with a refractive index ramp. We note that such effects are expected to be negligible if the original optical path gradients are achieved by only layer thickness ramps, i.e., if one chooses $n \times \Delta d$ (instead of $\Delta n \times d$, as in our case).

C. The analogy with a reverse-biased semiconductor diode

Due to an enhanced sensitivity to the changes of the refractive index gradients, an optical superlattice with resonant Zener tunneling acts as a carefully balanced photonic structure. The tuning of the photonic bands towards resonant coupling has an effect on light transmission that closely resembles the Zener tunneling of charge carriers in semiconductor diodes. In Fig. 5 we report the peak amplitude of the light transmission at the resonant Zener tunneling wavelength as a function of the gradient of the refractive index. The plot shows a threshold-like character, staying almost constant over a range of gradients and undergoing an enhancement once the critical gradient value of $\sim 10.1\%$ is reached. A transmission enhancement by a factor of 5 is reached after 300 ms of vapor exposure.

The optical superlattice at resonant Zener tunneling is extremely sensitive to vapor induced refractive index changes and therefore can be utilized for gas sensing. A careful design of the layer porosity (refractive index) gradient can be tailored to the critical radius of capillary condensation for various vapors, in order to maximize the tunability range and/or sensing properties of the optical superlattice upon choosing the proper direction of exposure. In addition, enhanced sensing of specific molecules can be achieved if one functionalizes the surface of the mesoporous silicon layers. Finally, our experiments show both perfect reversibility and reproducibility, which can guarantee the functionality of a long-life optical device.

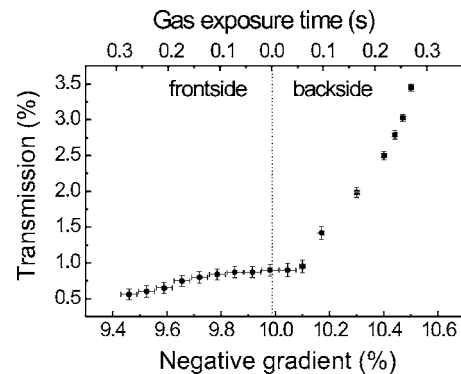


FIG. 5. Resonant Zener breakdown of the optical superlattice. With an increase in the optical path gradient along the sample, the light transmission shows a threshold-like behavior, in a close analogy to the tunneling current of electrons in a reverse-biased solid-state diode.

IV. CONCLUSIONS

In conclusion, we have demonstrated tunable tilting of photonic bands inside a porous optical superlattice exposed to organic vapor flows. The described sensitivity of vapor diffusion and/or condensation to the flow direction is specific for an optical superlattice made of a mesoporous material with a refractive index gradient. The described phenomenon could find future applications in optical sensing, switching, and processing.

ACKNOWLEDGMENTS

The authors wish to thank C. Toninelli, R. Sapienza, C.J. Oton, and P. Bettotti for interesting discussions. The authors acknowledge the financial support by MIUR through FIRB (RBNE01P4JF and RBNE012N3X) and COFIN (2004023725) projects, and IST-2-511616-NoE (EU NoE Phoremest).

-
- ¹M. F. Yanik, W. Suh, Z. Wang, and S. Fan, *Phys. Rev. Lett.* **93**, 233903 (2004); B. I. Mantsyzov, I. V. Melnikov, and J. S. Aitchison, *Phys. Rev. E* **69**, 055602(R) (2004); M. L. Povinelli, S. G. Johnson, and J. D. Joannopoulos, *Opt. Express* **13**, 7145 (2005).
- ²K. Busch and S. John, *Phys. Rev. Lett.* **83**, 967 (1998); X. Hu, Y. Liu, J. Tian, B. Cheng, and D. Zhang, *Appl. Phys. Lett.* **86**, 121102 (2005).
- ³R. Sapienza, P. Costantino, D. Wiersma, M. Ghulinyan, C. J. Oton, and L. Pavesi, *Phys. Rev. Lett.* **91**, 263902 (2003).
- ⁴M. Ghulinyan, C. J. Oton, Z. Gaburro, L. Pavesi, C. Toninelli, and D. S. Wiersma, *Phys. Rev. Lett.* **94**, 127401 (2005).
- ⁵T. F. Krauss, R. M. De La Rue, and S. Brand, *Nature (London)* **383**, 699 (1996); Sh.-Yu Lin, E. Chow, V. Hietala, P. R. Villeneuve, and J. D. Joannopoulos, *Science* **282**, 274 (1998).
- ⁶S. J. Gregg and K. S. V. Singh, *Adsorption, Surface Area and Porosity* (Academic, New York, 1982).
- ⁷Z. Gaburro, N. Daldosso, L. Pavesi, G. Faglia, C. Baratto, and G. Sberveglieri, *Appl. Phys. Lett.* **78**, 3744 (2001); Y. Y. Li, F. Cunin, J. R. Link, T. Gao, R. E. Betts, S. H. Reiver, V. Chin, S. N. Bhatia, and M. J. Sailor, *Science* **299**, 2045 (2003).
- ⁸W. Thomson, *Proc. R. Soc. Edinburgh* **7**, 63 (1870); **42**, 448 (1871).
- ⁹See EPAPS Document No. E-PRBMDO-74-036628 for a real-time movie demonstrating the tuning and detuning of resonant Zener tunneling of light when the vapor exposure is On and Off. This document can be reached via a direct link in the online article's HTML reference section or via the EPAPS homepage (<http://www.aip.org/pubservs/epaps.html>).
- ¹⁰M. Jona-Lasinio, O. Morsch, M. Cristiani, N. Malossi, J. H. Müller, E. Courtade, M. Anderlini, and E. Arimondo, *Phys. Rev. Lett.* **91**, 230406 (2003); V. V. Konotop, P. G. Kevrekidis, and M. Salerno, *Phys. Rev. A* **72**, 023611 (2005).
- ¹¹H. Trompeter, T. Pertsch, F. Lederer, D. Michaelis, U. Streppel, A. Bräuer, and U. Peschel, *Phys. Rev. Lett.* **96**, 023901 (2006); A. Fratallocchi, G. Assanto, Kasia A. Brzdukiewicz, and Mirek A. Karpierz, *Opt. Lett.* **31**, 790 (2006).
- ¹²H. Trompeter, W. Krolikowski, D. N. Neshev, A. S. Desyatnikov, A. A. Sukhorukov, Y. S. Kivshar, T. Pertsch, U. Peschel, and F. Lederer, *Phys. Rev. Lett.* **96**, 053903 (2006).
- ¹³G. H. Wannier, *Phys. Rev.* **100**, 1227 (1955).
- ¹⁴L. Esaki, *Phys. Rev.* **109**, 603 (1958).
- ¹⁵In our specific case, reported in Ref. 4, an increase in the light transmission by two orders of magnitude (from $\sim 0.3\%$ to 43%) has been observed.
- ¹⁶M. Ghulinyan, C. J. Oton, G. Bonetti, Z. Gaburro, and L. Pavesi, *J. Appl. Phys.* **93**, 9724 (2003).
- ¹⁷The choice of ZT frequency of the samples is a trade off between the absorption of our Si-based samples and the responsivity of the detection apparatus. This results in lower transmission values than those reported earlier for near infrared frequencies (Ref. 4).
- ¹⁸B. Coasne, A. Grosman, C. Ortega, and M. Simon, *Phys. Rev. Lett.* **88**, 256102 (2002).
- ¹⁹L. H. Cohan, *J. Am. Chem. Soc.* **60**, 433 (1938).
- ²⁰J. B. Pendry, *Adv. Phys.* **43**, 461 (1994).
- ²¹M. Knudsen, *Ann. Phys.* **28**, 75 (1909).
- ²²R. Valiullin, P. Kortunov, J. Kärger, and V. Timoshenko, *J. Appl. Phys.* **120**, 11804 (2004).